

Printed Band-Stop Filter for Mitigation of Electromagnetic Interference

Anjini Kumar Tiwary^{ID}, Nisha Gupta^{ID}

Department of ECE, Birla Institute of Technology, Mesra, Ranchi, Jharkhand, India

Cite this article as: A.K. Tiwary, N. Gupta, "Printed Band-stop Filter for Mitigation of Electromagnetic Interference", *Electrica*, vol. 21, no. 3, pp. 298-304, Sep. 2021..

ABSTRACT

A new printed microstrip band-stop filter is proposed and implemented. A systematic design approach is presented to realize the filter for a specific band of operation employing the concept of SIR and embedded stub. The proposed filter design is suitable for multiple stop band applications. Moreover, the filter configuration can be easily incorporated in the microstrip feed line connected with a radiating element to reject the signal at the desired band for mitigating the electromagnetic interference. A prototype model of the proposed design is developed, and characteristics are measured and compared with the simulation result. A good agreement between the two is evident.

Index Terms—Band-stop filter embedded stub, microstrip filter, stepped impedance resonator

Corresponding Author:

Anjini Kumar Tiwary

E-mail:

aktiwary@bitmesra.ac.in

Received: February 15, 2021

Accepted: June 2, 2021

Available Online Date: August 27, 2021

DOI: 10.5152/electrica.2021.21018

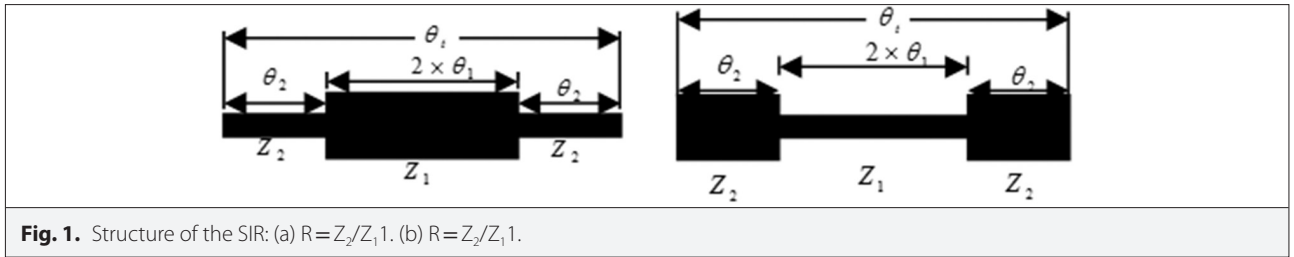


Content of this journal is licensed under a Creative Commons Attribution-NonCommercial 4.0 International License.

I. INTRODUCTION

The printed filter configurations capable of multiband operation are becoming key aspect of various communication systems. Among the various filter configurations, the band-stop filters (BSF) find application for the mitigation of electromagnetic interference (EMI) [1-3]. In fact, these filters are used when it is required to attenuate the interfering signals transmitted from other communication systems impinging the frequency band at specific locations. In the absence of such a filter, the performance of the communication device deteriorates due to interference. The BSFs can be easily realized by using a serial transmission line with a quarter wavelength stub [4-6] which introduces transmission zeros. A compact fifth-order single-ended BPF with multiple transmission zeros introduced to improve its performance is presented in [7]. A compact BSF [8] using parallel coupled lines and open stubs with four transmission poles is realized with good roll-off skirts and stop band-suppression characteristics. A stepped impedance resonator (SIR) [9] is used in the design and analysis of a planar BSF to extend its upper passbands and improve the return loss in passband. The structure shows band-stop filtering performance. A planar BSF [10] is implemented with the help of L-shaped open stubs and a T-Shaped SIR which is used to transmit and receive parts in the RF-system. The BSF configuration can also be realized by embedding the stub in the transmission line itself or by etching a spur line in the transmission line [11, 12]. However, both methods used to realize a BSF configuration pose fabrication problems due to stringent dimension tolerances. Moreover, the high impedance lines employed have higher dissipation loss along with structural technological constraints. The proposed design is capable of alleviating this problem to a certain extent by realizing the embedded stub, based on the SIR concept, thus providing more degrees of freedom in design. A similar concept has been presented in [13] but with a different approach based on the computation of the equivalent characteristic impedance through simulation.

In the present approach, the impedance of the stubs is interpreted from the simulation result obtained from the embedded filter as a whole. The proposed method directly calculates the embedded filter parameters from the SIR formula or the graph. To demonstrate



this design concept, a prototype model is developed, and the simulation and experimental results are presented for a typical configuration.

II. FILTER DESIGN

The design of the embedded stub is based on the SIR concept. The schematic of a typical half-wavelength SIR is shown in Fig. 1. The input admittance Y_i from an open end is given as [14], where θ_1 , and θ_2 are the electrical lengths specified in the structure of SIR, as shown in Fig. 1(a) and (b):

$$Y_i = \frac{2(R \tan \theta_1 + \tan \theta_2)(R - \tan \theta_1 \tan \theta_2)}{R(1 - \tan^2 \theta_1)(1 - \tan^2 \theta_2) - 2(1 + R^2) \tan \theta_1 \tan \theta_2} \quad (1)$$

To determine the resonance conditions of the SIR, one needs to substitute the value of $Y_i = 0$. Thus, the resonance condition is obtained as:

$$R = \frac{Z_2}{Z_1} = \tan \theta_1 \tan \theta_2 \quad (2)$$

and can be designated by the equation:

$$R \cot \theta_2 = \tan \theta_1 \text{ or } -\cot \theta_1 \quad (3)$$

The degree of freedom in the design is highly recommended to overcome the stringent fabrication constraints, and this can be conveniently increased by varying the impedance ratio (R) and the length ratio (α) of the SIR to adjust the higher-order resonant modes. The length ratio (α) is defined as [14]:

$$\alpha = \frac{2\theta_2}{\theta_t} = \frac{2\theta_2}{2(\theta_1 + \theta_2)} = \frac{\theta_2}{\theta_1 + \theta_2} \quad (4)$$

where θ_t is the total electrical length of the SIR, and is represented by θ_t as shown in Fig. 1.

From (2) and (3) we get:

$$R \cot \left[\frac{\alpha \times \theta_t}{2} \right] = \tan \left[\frac{(1 - \alpha) \times \theta_t}{2} \right] \quad (5)$$

Choice of α and impedance ratio R [15] give rise to various solutions of resonant electrical length, as shown in Fig. 2. The first spurious resonance frequency f_{s1} is given by:

$$f_{s1} = \frac{\pi}{2 \tan^{-1}(\sqrt{R})} f_0 \quad (6)$$

where, f_0 is the resonant frequency of the SIR.

The geometrical configuration of an open circuited single-section stub consists of a 50Ω microstrip line connected to a shunt stub, where W is the width of the microstrip line, and W_1 is the width of the shunt stub as, shown in Fig. 3 (a).

A compact configuration of this open-circuited stub can be realized easily by embedding the stub in the 50Ω microstrip line along its length, as shown in Fig. 3(b). Here, W_1 is the strip width of the embedded stub, W is the width of the microstrip line, and W_2 is the width of the embedding structure. The dimensions W and W_2 are kept fixed while W_1 can be varied. Fig. 3(c) shows the embedded two-section stub which has the effective length of a quarter wavelength at the normalized frequency [11,12].

In the proposed structure, the embedded stub is a simple SIR configuration with the impedance ratio $R < 1$, as shown in Fig. 4.

The value of R is selected based on the data (Z_2/Z_1) to be used for fabrication of the embedded SIR band-stop filter.

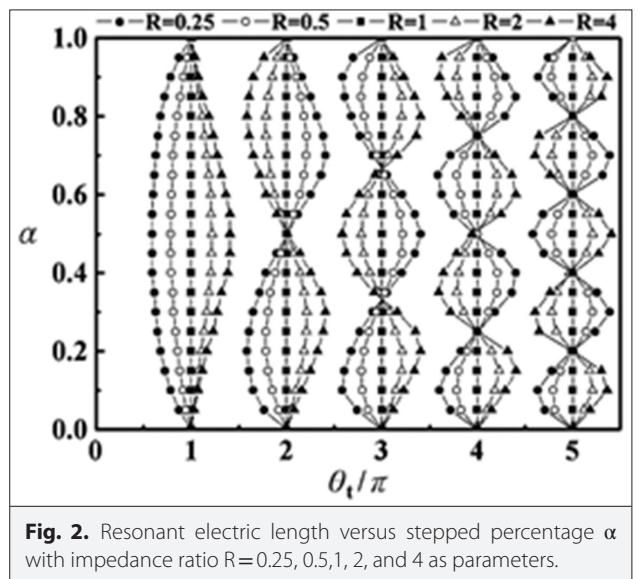


Fig. 2. Resonant electric length versus stepped percentage α with impedance ratio $R=0.25, 0.5, 1, 2,$ and 4 as parameters.

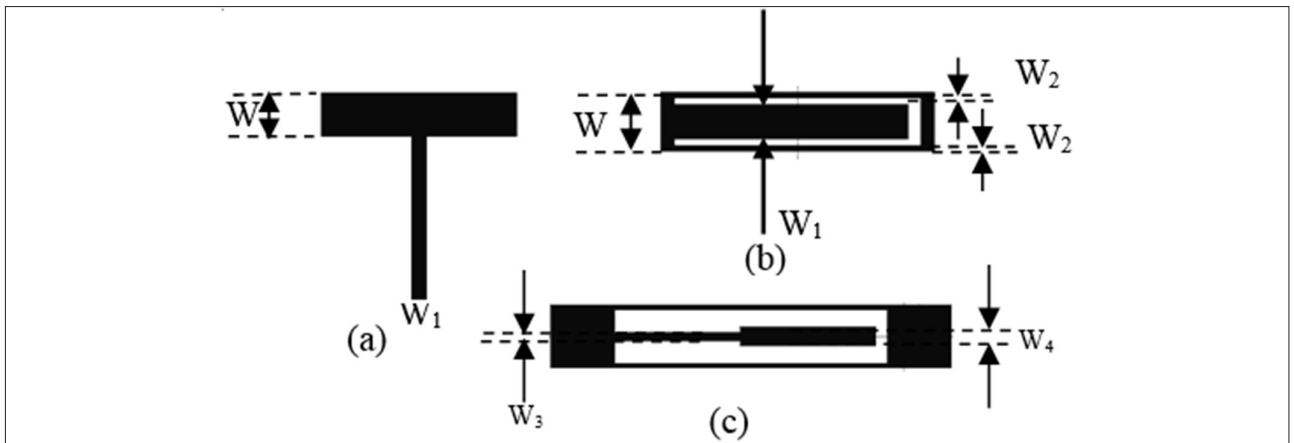


Fig. 3. Open-circuited stub:(a) conventional stub (b) embedded stub (c) embedded two-section stub.

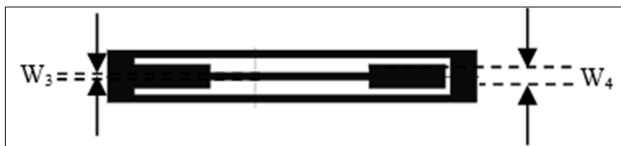


Fig. 4. Embedded SIR stub in the proposed BSF.

The available fabrication facility allows the value of the ratio (Z_2/Z_1) greater than or equal to 0.625 and less than 1, which in turn fixes up the value of R for a particular case. The proposed SIR configuration thus offers an added advantage of flexible selection of the R parameter. Additionally, it can be simply used as the feed of a radiating element [16] to reject any undesired signal at the specific locations interfering in the desired band.

III. SIMULATED AND EXPERIMENTAL RESULTS

The proposed BSF structure is simulated using a full-wave method of moments (MOM) simulation software package IE3D from Zeland [17]. The design of the embedded structure is implemented on an FR4 substrate with $\epsilon_r=4.4$, thickness of 1.6 mm, and loss tangent of 0.016. Considering these substrate parameters, the strip-width W of the 50 Ω microstrip line is obtained as 3.06 mm, while the width W_2 is set to a fixed value of 0.4 mm. The width W_2 is chosen judiciously so that it attains a moderate value that is neither very large nor very small. In case W_2 is selected to be small, it may introduce unwanted losses; if it is chosen to be large, it may limit the range of variation of W_1 . For every R ($0.625 < R < 1$) there are various values of length ratio (α), as shown in Fig. 2. The value of $\lambda_g = 108.8$ mm corresponds to $f_o = 1.5$ GHz. Three SIR configurations are considered in the design, and the various parameters are listed in Table I. The simulation results for the best cases are shown in Fig. 5.

It is observed that with the increase in impedance ratio, the total length of the SIR filter also increases and 3-dB bandwidth decreases. Hence, for the minimization of SIR filter size, the

impedance ratio (R) should be low, that is, 0.625 (the optimum impedance ratio). Moreover, (6) clearly indicates that for a lower impedance ratio, the first spurious frequency moves farthest from the resonant frequency.

Next, the filter configuration is simulated to examine the S-parameter characteristics. Fig. 5 depicts the simulation results of reflection and insertion loss characteristics. As evident, two stop-bands occur at frequencies 0.9 GHz and 2.94 GHz, possessing bandwidths of 0.37 GHz and 0.45 GHz respectively.

Again, the simulation results for optimum impedance ratio ($R=0.625$), considering different sets of length ratio (α), are listed in Table II.

It is observed that the total optimized length is the lowest for stepped percentage $\alpha=0.4902$ and $R=0.625$.

Next, to examine the in-band and out-of-band (passband) characteristics of the proposed filter, the current distribution is plotted, shown in Fig. 6.

The current distribution is shown in Fig. 6(a)–(c) in the in-band and Fig. 6(d)–(e) in the out-of-band. From the current distribution plot, it is clear that the first three resonances are due to the excitation of the longitudinal modes along the length of the microstrip line. To validate the design concept, a prototype model of the SIR band-stop filter is fabricated, as shown in Fig. 7.

Next, the simulation results are compared with the measured results, as shown in Fig. 8, which indicates a good agreement between the two. Finally, the performance of the proposed filter is compared with the state-of-the-art filter structures available in the literature, and presented in Table III for comparisons. As evident, the proposed filter offers a compact structure even at a lower operating frequency.

TABLE I. DESIGN PARAMETERS OF THE SIR

	SIR 1	SIR 2	SIR 3
Impedance ratio $R = Z_2/Z_1$	0.625 = 75/120	0.75 = 90/120	0.89 = 106.8/120
Stepped percentage α	0.4902	0.49	0.48
Width of Z_2 (mm)= W_4	1.4320	0.9368	0.5876
Width of Z_1 (mm)= W_3	0.4084	0.4084	0.4084
Stepped section length l_2 (mm)	11.357	12.113	12.573
Central section length $2l_1$ (mm)	23.622	25.214	27.241
Total length of the SIR (i.e., $\theta_t = 2l_1 + 2l_2$ (mm))	46.337	49.44	52.387
First stop-band f_0 (GHz)	0.9	0.875	0.85
Second stop-band f_{s1} (GHz)	2.95	2.725	2.575
Third stop-band f_{s2} (GHz)	4.78	4.52	4.291
3 dB Bandwidth (first stop-band)	0.151	0.147	0.13878

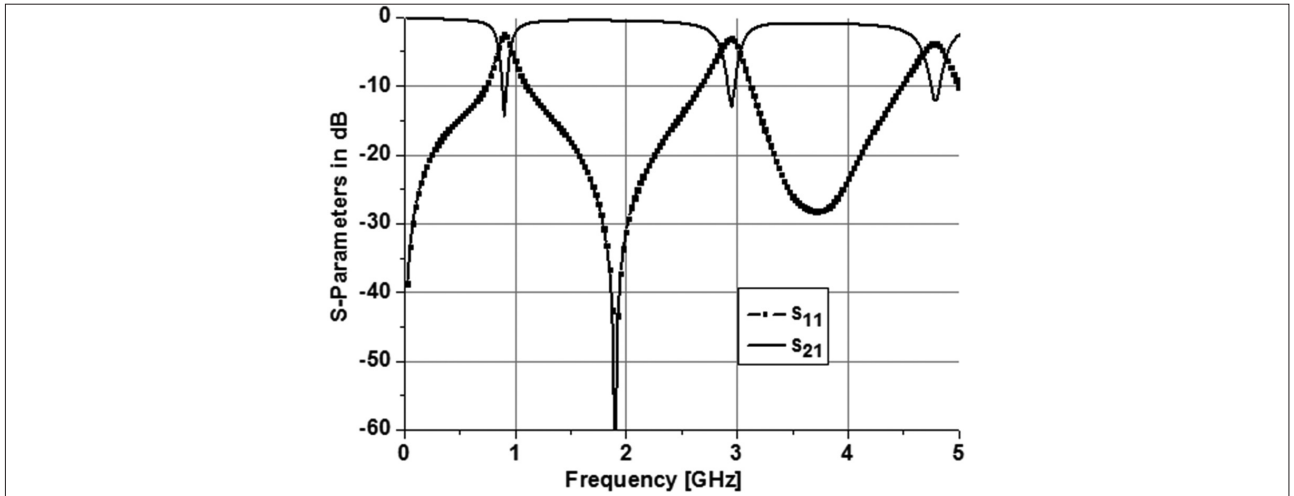


Fig. 5. Simulated S-parameter characteristics of the embedded SIR for the optimum impedance ratio (R) = 0.625.

TABLE II. COMPARATIVE STUDY OF THREE SIRS

	SIR 1	SIR 2	SIR 3
Impedance ratio $R = Z_2/Z_1$	0.625 = 75/120	0.625 = 75/120	0.625 = 75/120
Stepped percentage α	0.4902	0.3136	0.2574
Width of Z_2 (mm)	1.4320	1.4320	1.4320
Width of Z_1 (mm)	0.4084	0.4084	0.4084
Stepped section length l_2 (mm)	11.357	7.4287	6.193
Central section length $2l_1$ (mm)	23.622	32.52	35.736
Total length of the SIR (i.e., $\theta_t = 2l_1 + 2l_2$ (mm))	46.337	47.38	48.122

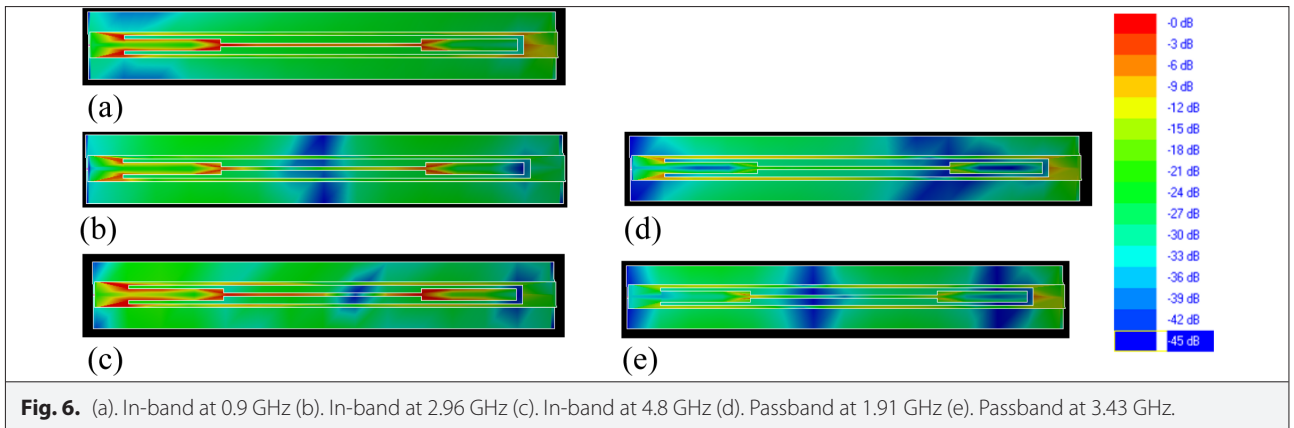
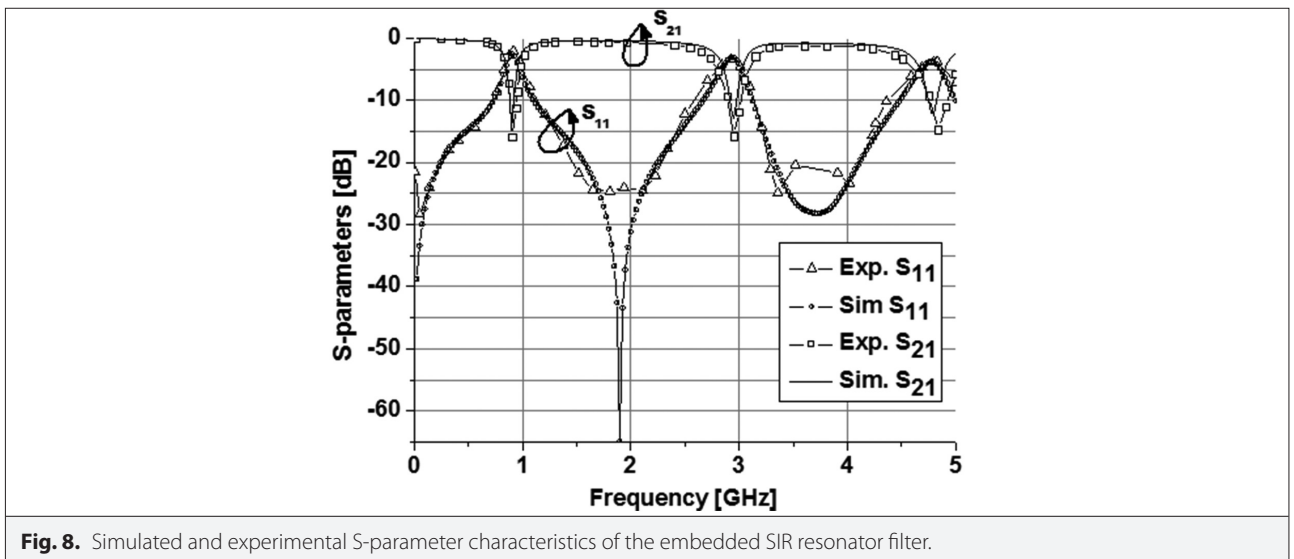


TABLE III. PERFORMANCE COMPARISONS WITH REPORTED FILTER STRUCTURES

Ref.	Operating Frequency in GHz	Band-stop Bandwidth ($ S_{21} < -20$ dB)	Lower Pass Band ($ S_{11} < -17$ dB)	Upper Pass Band ($ S_{11} < -17$ dB)	Size in mm ²	Method
[8]	1.75	0.05 GHz	-	-	47×22	stub
[11]	1.75	0.3 GHz	0.6–1.4 GHz	2.4–4.5 GHz	51×22.42	Transmission point
[12]	1.01	0.37 GHz	0–0.45 GHz	1.72–6.02 GHz	77.14×23.74	SIR
Proposed	0.9, 2.94, 4.8	0.37 GHz, 0.45 GHz at 10 dB	0–0.46 GHz	1.4–2.4 GHz, 3.2–4.2 GHz	3.06×46.33	SIR



IV. CONCLUSION

A novel design approach based on the SIR concept has been demonstrated for the purpose of designing a multi-band embedded BSF. The proposed design offers flexibility in selecting the desired ratio of impedances of the embedded SIR stub. The length of the stub can be varied, not just in terms of multiple of π , but other values that are also possible which can be interpreted from a θ_i versus α graph. The desired bandwidth corresponding to a specific stop band can be achieved by selecting the frequency approximately. The proposed design can easily be integrated with the radiating element of any printed antenna as its feeding element, for rejecting the desired frequencies to mitigate the electromagnetic interference.

Peer-review: Externally peer-reviewed.

Author Contributions: Concept – A.K.T.; Design – A.K.T.; Supervision – N.G.; Writing Manuscript – A.K.T., N.G.; Critical Review – A.K.T., N.G.

Conflict of Interest: The authors have no conflicts of interest to declare.

Financial Disclosure: The authors declared that this study has received no financial support.

REFERENCES

1. T. Hubing, "Printed circuit board EMI source mechanisms." IEEE Symposium on Electromagnetic Compatibility, Symposium Record, vol.1, , pp. 1–3, 2003.
2. S. Wu and Y. Lin, "A wideband noise-isolation bandstop power distribution network using quarter-wavelength line-based structure," *IEEE Transactions on Components, Packaging and Manufacturing Technology*, vol. 4, no. 6, pp. 1071–1081, 2014. [\[CrossRef\]](#)
3. A. K. Tiwary and N. Gupta, "Compact wide band printed filter with improved out-of-band performance," *Applied Computational Electromagnetics Society Journal*, vol. 29, pp. 224–230, 2014.
4. C.-W. Hsue, C.-W. Ling and W.-T. Hung, "Discrete-time notch filter and its application to microwave filter," *Microwave and Optical Technology Letters*, vol. 50, no. 6, pp. 1596–1600, 2008. [\[CrossRef\]](#)
5. M. Sagawa, M. Makimoto and S. Yamashita, "Geometrical structures and fundamental characteristics of microwave stepped-impedance resonators," *IEEE Transactions on Microwave Theory and Techniques*, vol. 45, no. 7, pp. 1078–1085, 1997. [\[CrossRef\]](#)
6. M. Makimoto and S. Yamashita, *Microwave Resonators and Filters for Wireless Communication Theory, Design and Application*. Germany: Springer-Verlag, 2001.
7. D. Li, Kai-Da. Xu and A. Zhang, "Single-ended and balanced band-pass filters using multiple pairs of coupled lines and stepped-impedance stubs," *IEEE Access*, vol. 8, pp. 13541–13548, 2020. [\[CrossRef\]](#)
8. Y. Cai, Kai-Da. Xu, Z. Ma and Y. Liu, "Compact bandstop filters using coupled lines and open/short stubs with multiple transmission poles," *IET Microwaves, Antennas & Propagation*, vol. 13, no. 9, pp. 1368–1372, 2019. [\[CrossRef\]](#)
9. X. Zuo and J. Yu, "A stepped-impedance bandstop filter with extended upper passbands and improved pass-band reflections," *AIP Advances*, vol. 6, no. 9, pp. 1–7, 2016. [\[CrossRef\]](#)
10. T. Lee, C. Kim, K. C. Son, K. S. Shin, B. Shrestha and K. Yoon, "A band-stop filter with wide stop band using T-shaped stepped impedance resonator and L-shaped open stub," International Conference on Emerging Trends & Innovation in ICT (ICEI), Vol. 2017, 2017, pp. 154–156.
11. C. W. Hsue, Y. H. Tsai and C. Y. Wu, "Bandstop filters with variable upper passbands using embedded line, spur line and conventional microstrip," *Microwave and Optical Technology Letters*, vol. 53, no. 8, pp. 1921–1924, 2011. [\[CrossRef\]](#)
12. C. W. Hsue, R. Mittra, Y. Tsai and C. C. Hsu, "Microwave notch filters using embedded stubs," *Microwave and Optical Technology Letters*, vol. 51, no. 12, pp. 2839–2842, 2009. [\[CrossRef\]](#)
13. L. Kumar and M. S. Parihar, "A wide stopband low-pass filter with high roll-off using stepped impedance resonators," *IEEE Microwave and Wireless Components Letters*, vol. 28, no. 5, pp. 404–406, 2018. [\[CrossRef\]](#)
14. A. Worapishet, K. Srisathit and W. Surakamponorn, "Stepped-impedance coupled resonators for implementation of parallel coupled microstrip filters with spurious band suppression," *IEEE Transactions on Microwave Theory and Techniques*, vol. 60, no. 6, pp. 1540–1548, 2012. [\[CrossRef\]](#)
15. C.-F. Chen, T.Y. Huang and R.-B. Wu, "Compact microstrip cross-coupled bandpass filters using miniaturized stepped impedance resonators," *Proceedings Asia-Pacific Microwave Conference*, Vol. 2005, 2005, p. 4.
16. M. M. Hosain, S. Kumari and A. K. Tiwary, "Sunflower shaped fractal filtenna for WLAN and ARN application," *Microwave and Optical Technology Letters*, vol. 62, no. 1, pp. 346–354, 2020. [\[CrossRef\]](#)
17. IE, *3D Simulator*. Fremont, CA: Zeland Software Inc., 1997.



Anjini Kumar Tiwary was born in Jamshedpur, India in 1972. He received an M.E. degree and Ph.D. degree from Birla Institute of Technology, Ranchi, India in 2009 and 2013, respectively. Currently, he is an Assistant Professor for the Department of Electronics and Communication Engineering, Birla Institute of Technology, Ranchi, India. He has authored and co-authored more than 20 technical journal articles. His research interests are microstrip filter design, microwave metamaterials and its applications in antenna and filter, and filtenna and its applications in wireless devices.



Nisha Gupta received Bachelor's and Master's degrees in Electronics Telecommunication and Electrical and Electronics Engineering both from Birla Institute of Technology, Mesra, Ranchi, India and also a Ph.D. degree from the Indian Institute of Technology, Kharagpur, India. She was a Maintenance Engineer at Shreeram Bearings Ltd., Ranchi from 1982 to 83 and a Programmer at Ranchi University, Ranchi from 1983 to 1986. She was a Junior Scientific Officer in a DRDO-sponsored project at the Department of Electronics and Electrical Communication Engineering, Indian Institute of Technology, Kharagpur, from 1986 to 1989 and an Institute Research Scholar and Research Associate (CSIR) in the same department from 1990 to 1996. She was a post-doctoral fellow at the University of Manitoba, Canada from 1997 to 1998 before joining the Department of Electronics and Communication Engineering, Birla Institute of Technology in 1999 as a reader. Currently, she is a Professor and Head in the same department. She has authored and co-authored more than 105 technical journal articles. Her research interests are computational electromagnetics, RF circuits and antennas for wireless communication and AI techniques in wireless and mobile communication.